#### CHAPTER IV

## RESULTS AND DISCUSSION

In chapter III, we presented the modeling of the calibration neutron monitor using the FLUKA program with Monte Carlo method including the characteristics of beam. In the simulation, we developed the technique of weight beam of atmospheric secondary particles.

In this chapter, we show the simulation results in 3 main sections which are distribution of particle energy, count rate as a function of height of calibration monitor and water below it, and count rates inside and outside the PSNM station.

Distribution of particle energy in the calibration monitor and the neutron monitor

### 1. in the calibration monitor

0

We simulated the calibration monitor by using the input data of 10 million secondary particles with the weight beam. The data files were generated by John Clem for the PSNM station. We found that the simulation results of some particles had the count rate more than the experimental results because this count rate included the reflected particles from the ground into the CALMON. Therefore, we developed the ratio of new weights from new flux (J<sub>PSM</sub>) of the secondary particles, which were applied by Pierre-Simon Mangeard, and were divided by old flux from John Clem (J<sub>JC</sub>) for each energy and 9 types of particles (neutron, proton, muon(+), muon(-), pion(+), pion(-), photon, electron and positron) to be new weights. Where

weight = 
$$\frac{J_{PSM}}{J_{JC}}$$
 (10)

and Ni is the number of counts in each run

$$N_i = Counts_{per file} = \sum_{i=1}^{N_{counts}} 1 \times W_{area} \times \frac{J_{PSM}(type,Ek)}{J_{JC}(type,Ek)}$$

: }

the ratio of CAL/NM = 
$$\frac{\overline{N}_{CAL}}{\overline{N}_{NM}}$$
 (11)

From the simulation results, we plotted the energy distributions in the calibration monitor for the various particles as a function of log (kinetic energy) as shown in Figure 36-44. The Figure 45-53 show the distributions of energies in the neutron monitor when x-axis is log scale of energy in GeV and y-axis is the number of counts in counts cm<sup>-2</sup>s<sup>-1</sup>

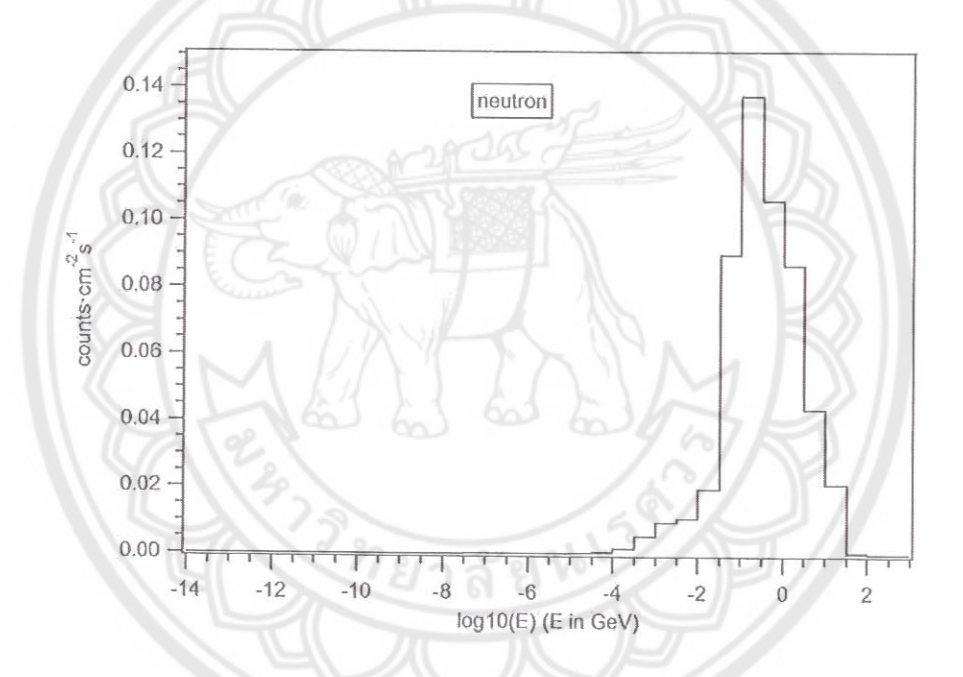


Figure 36 Distribution of counts issued by secondary neutron in the calibration monitor.

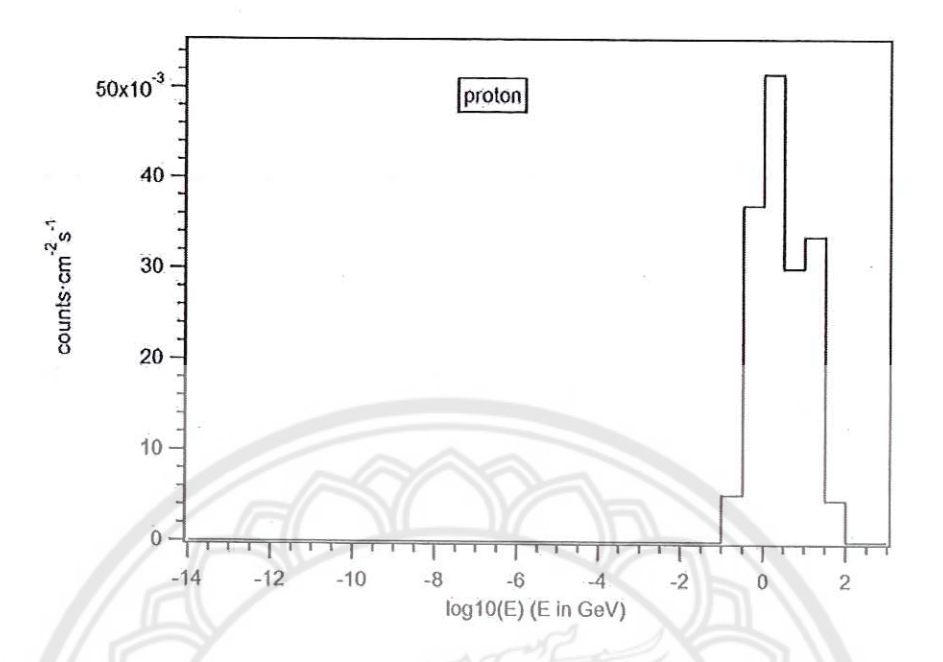


Figure 37 Distribution of counts issued by secondary proton in the calibration monitor.

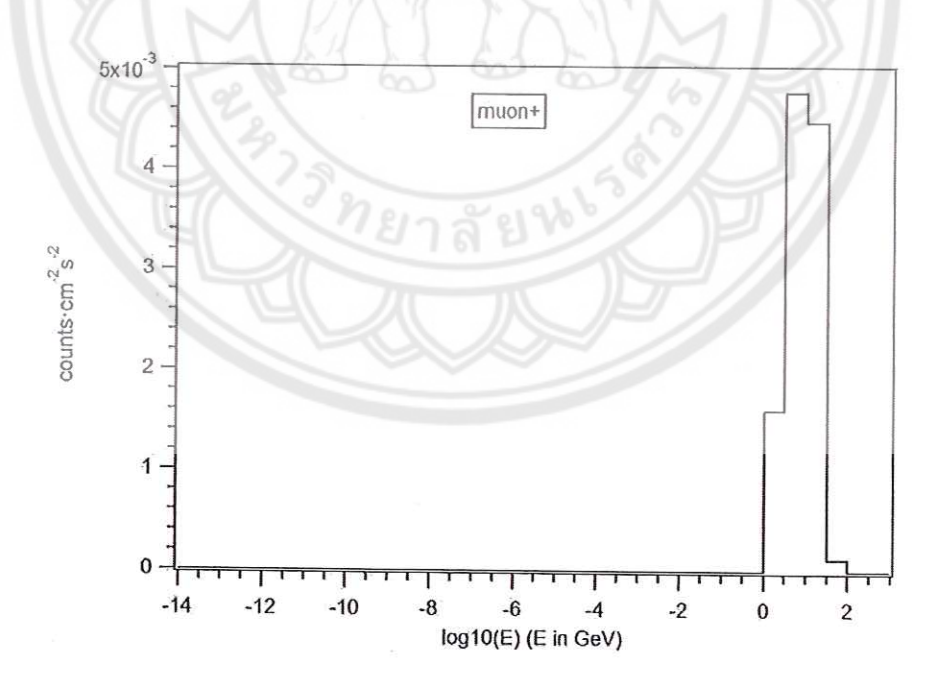


Figure 38 Distribution of counts issued by secondary muon(+) in the calibration monitor.

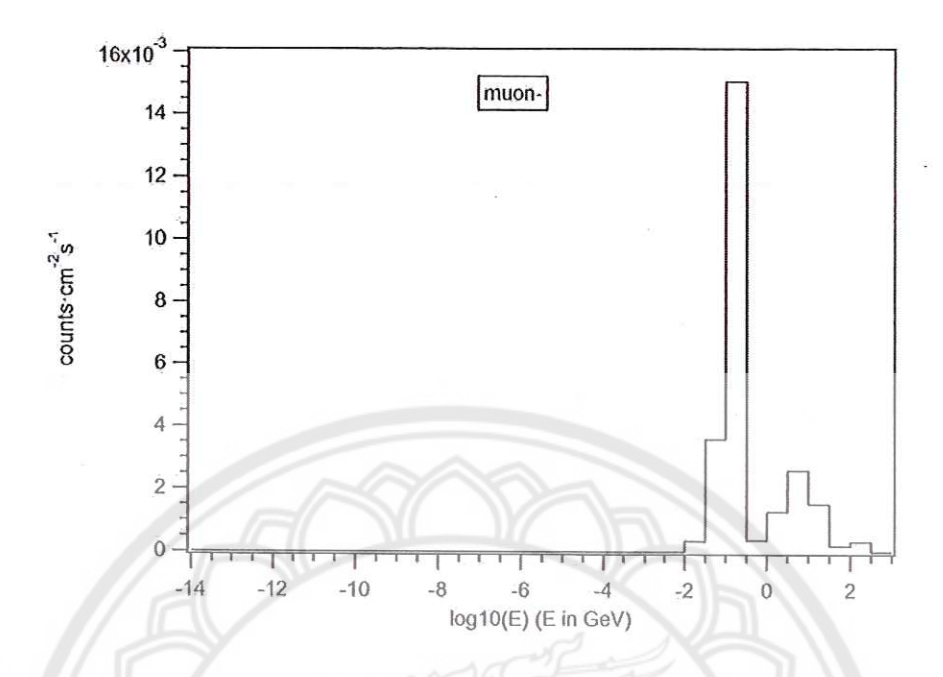


Figure 39 Distribution of counts issued by secondary muon(-) in the calibration monitor.

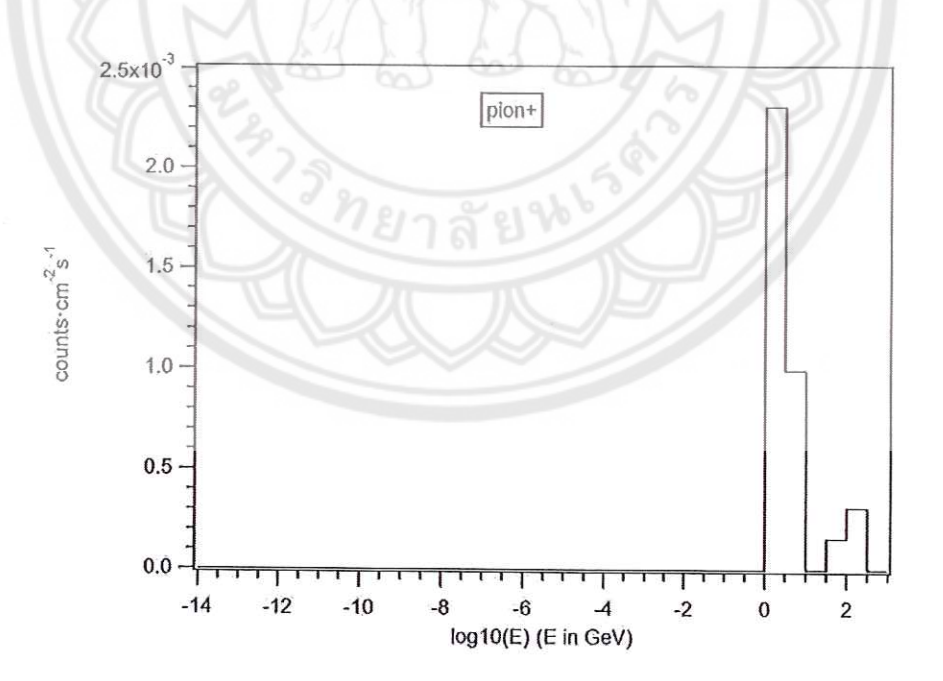


Figure 40 Distribution of counts issued by secondary pion(+) in the calibration monitor.

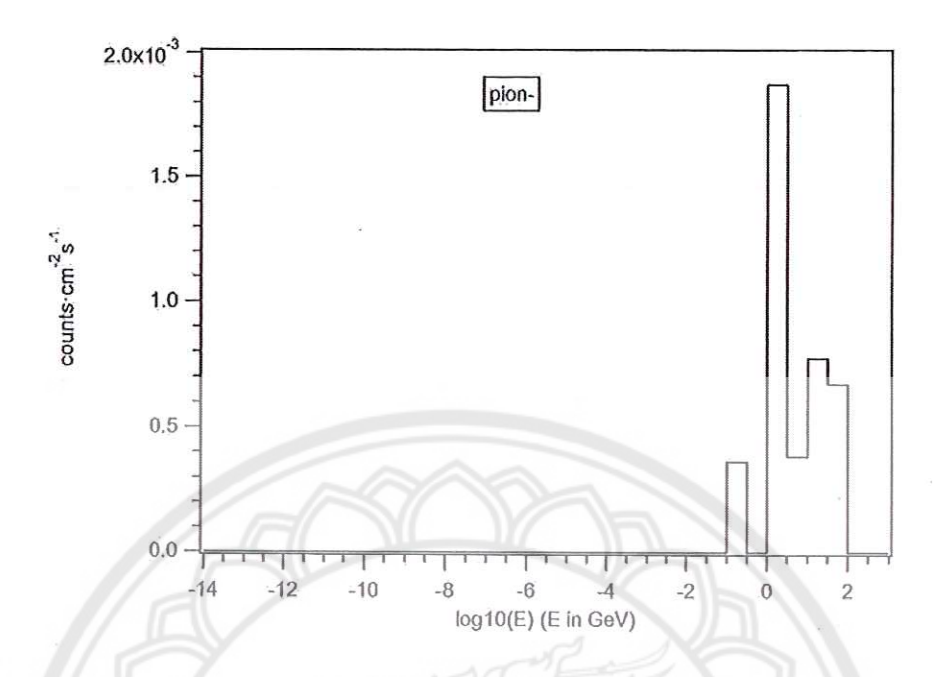


Figure 41 Distribution of counts issued by secondary pion(-) in the calibration monitor.

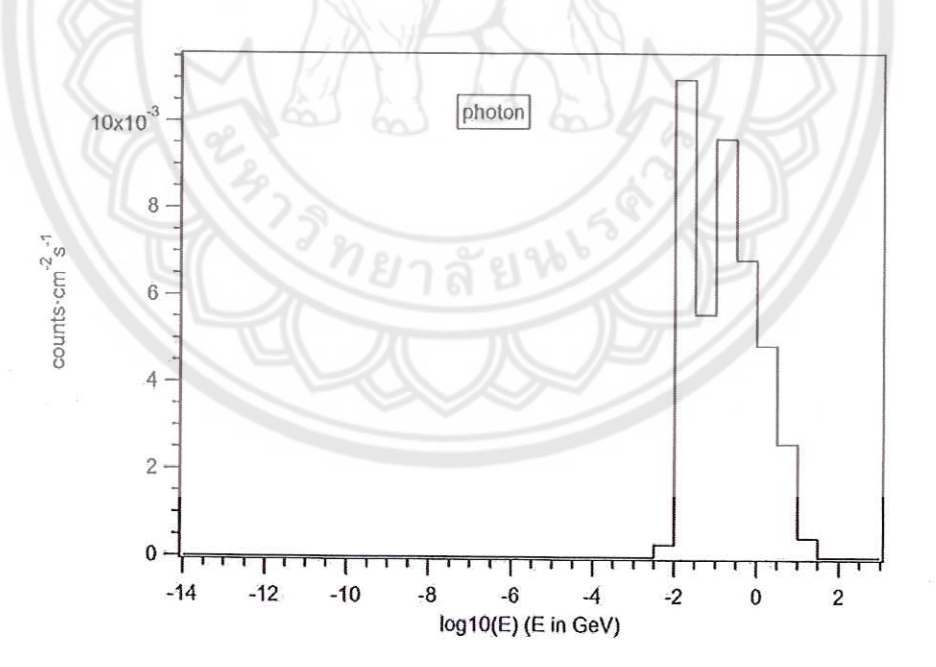


Figure 42 Distribution of counts issued by secondary photon in the calibration monitor.

3.

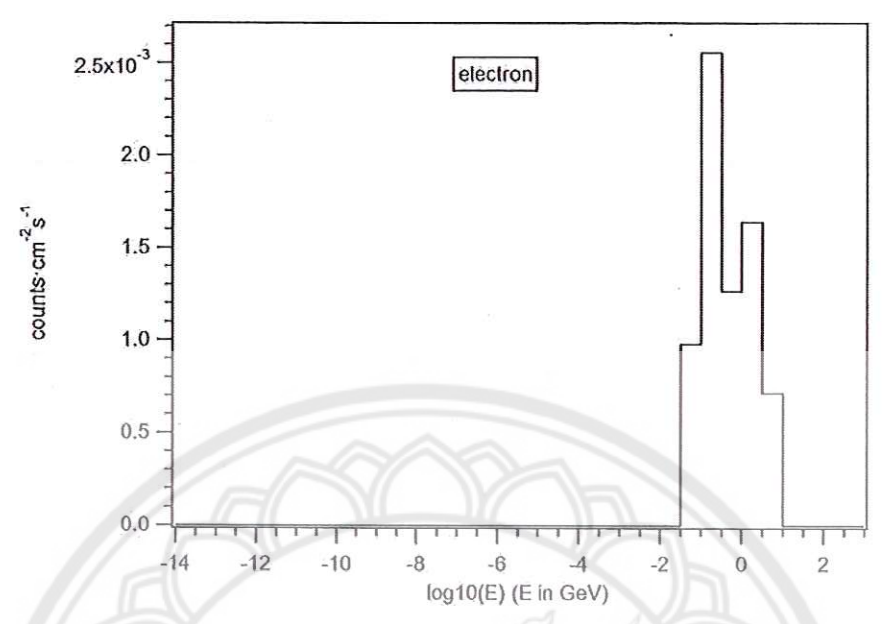


Figure 43 Distribution of counts issued by secondary electron in the calibration monitor.

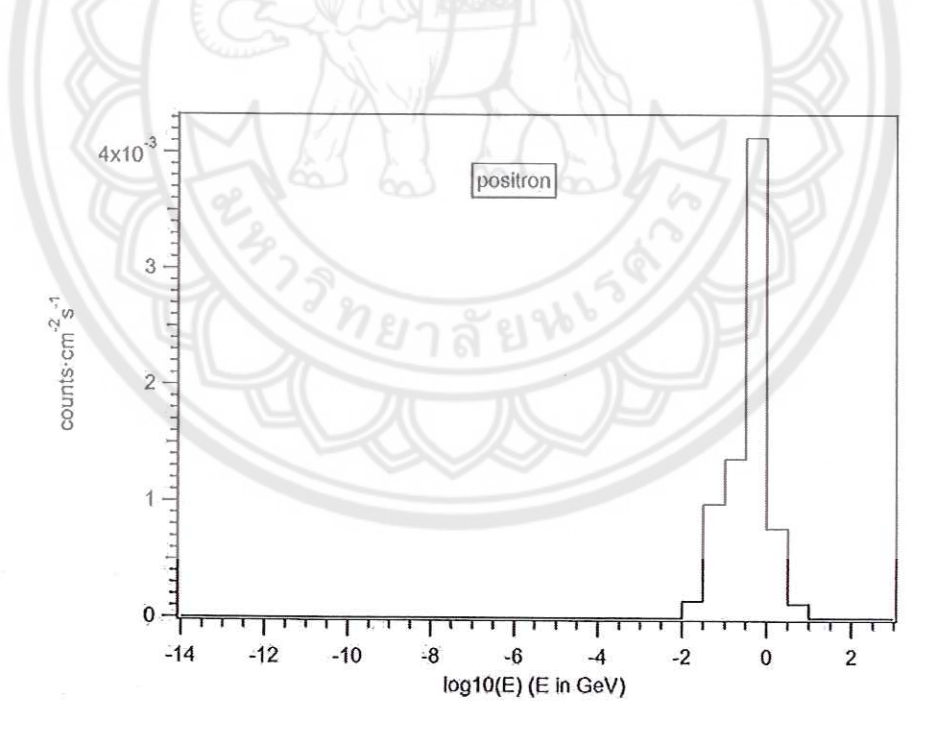


Figure 44 Distribution of counts issued by secondary positron in the calibration monitor.

?

# 2. in the neutron monitor

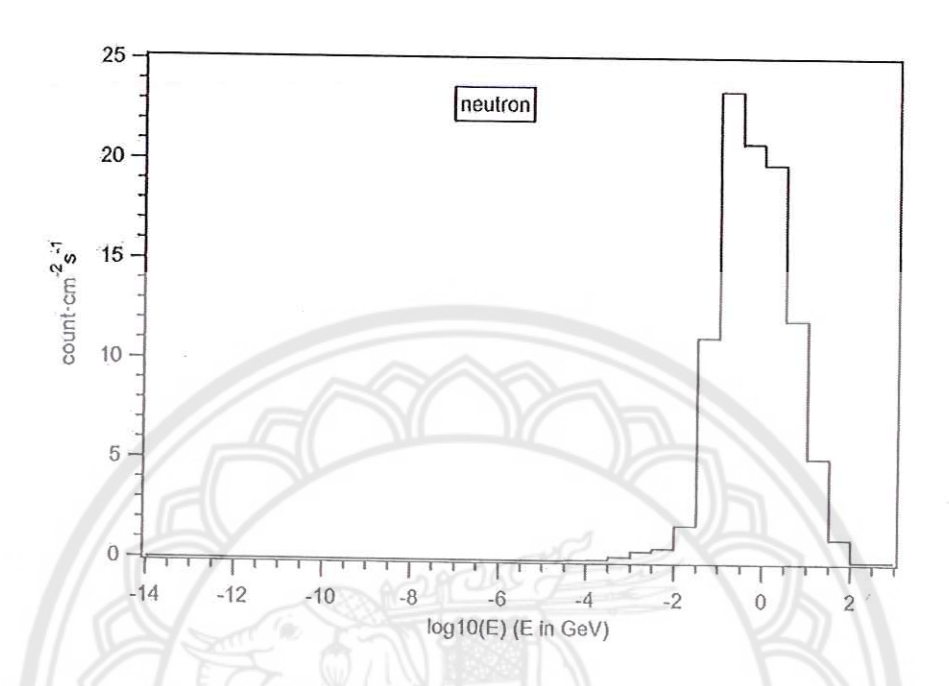


Figure 45 Distribution of counts issued by secondary neutron in the neutron monitor.

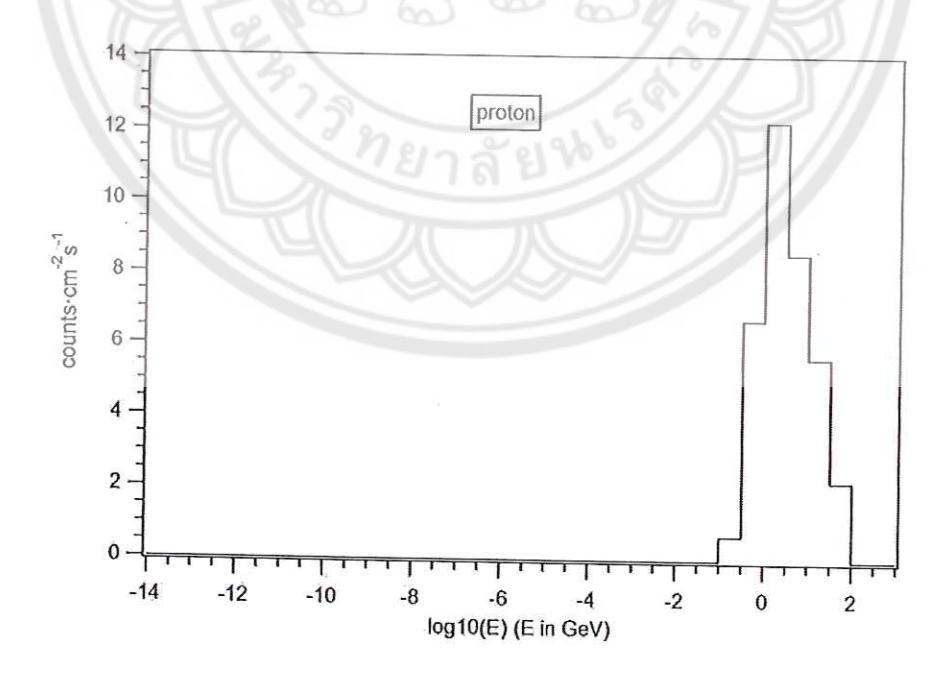


Figure 46 Distribution of counts issued by secondary proton in the neutron monitor.

()

)

- 23

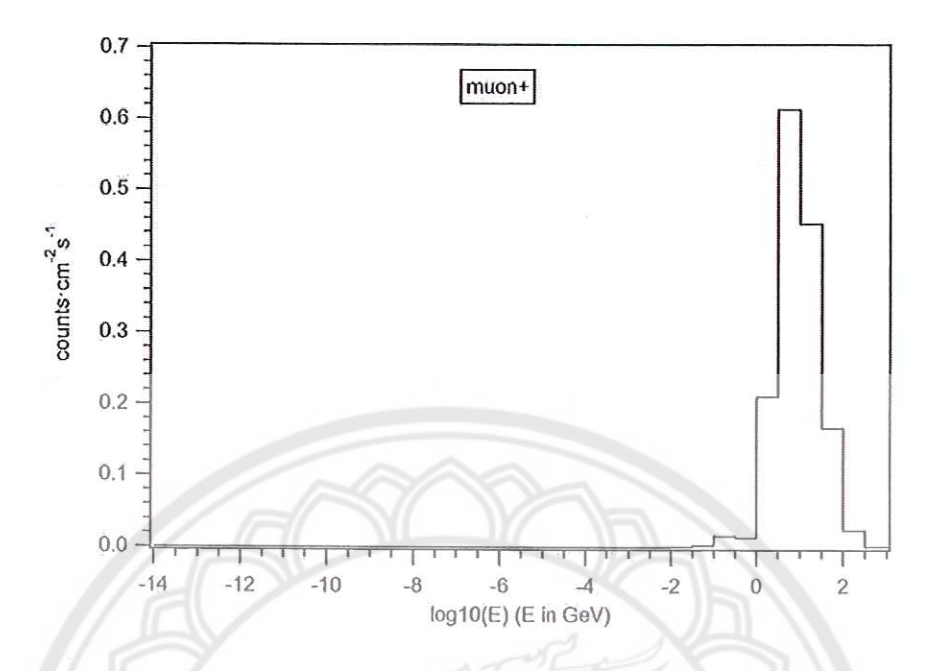


Figure 47 Distribution of counts issued by secondary muon (+) in the neutron monitor.

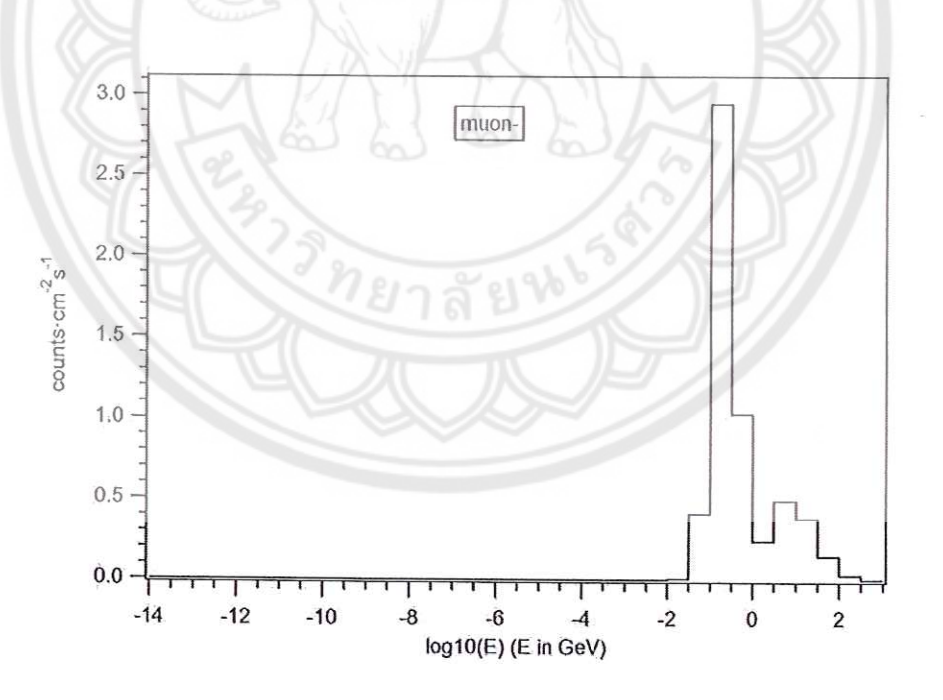


Figure 48 Distribution of counts issued by secondary muon (-) in the neutron monitor.

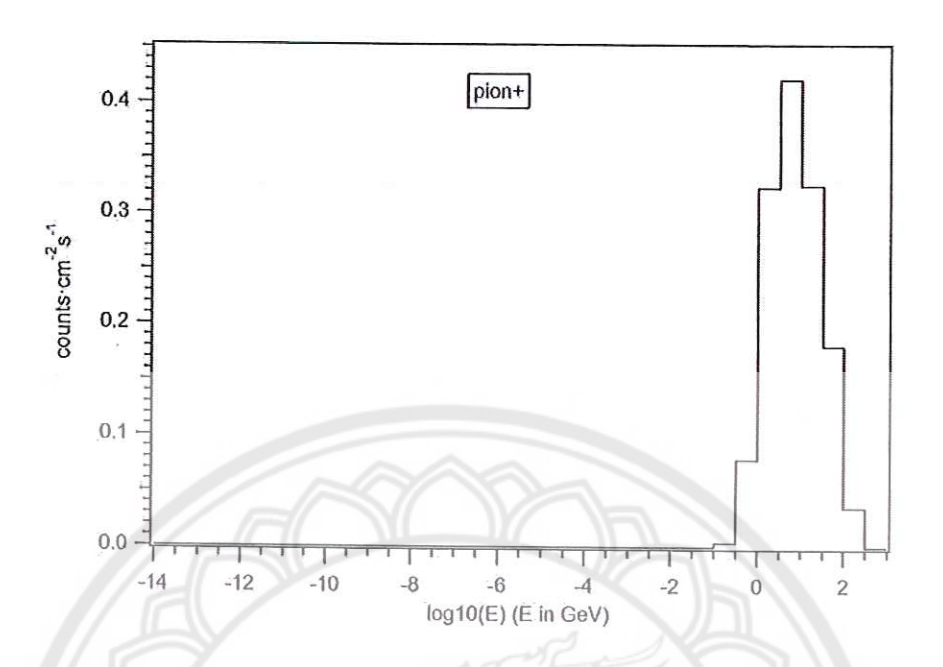


Figure 49 Distribution of counts issued by secondary pion (+) in the neutron monitor.

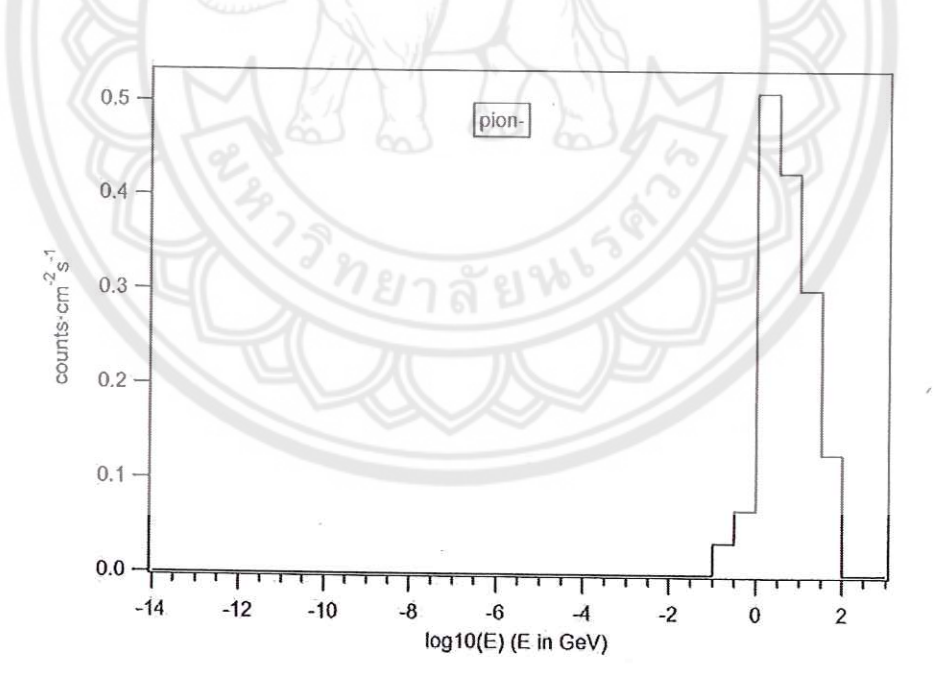
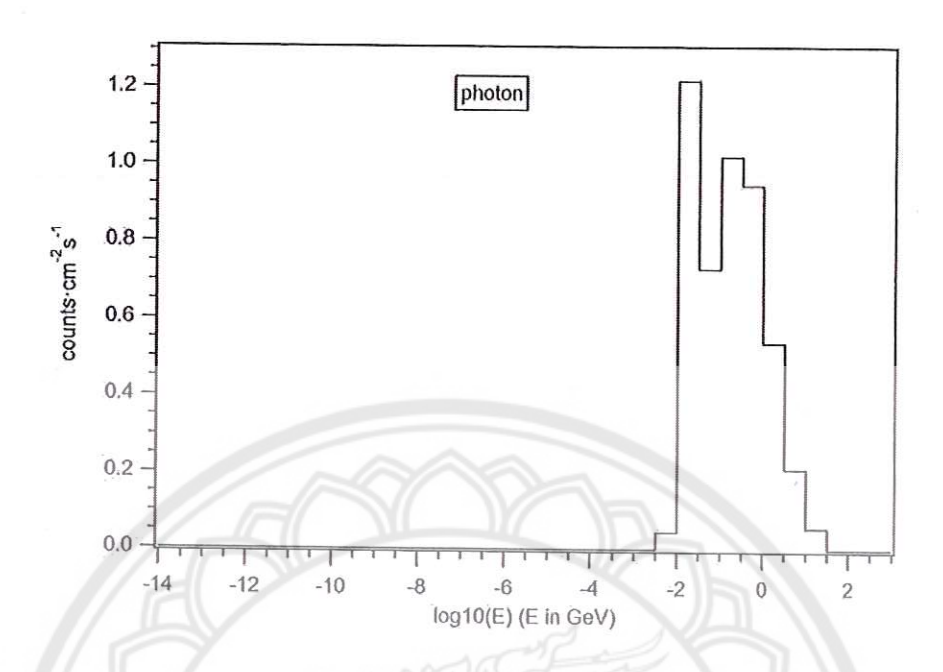


Figure 50 Distribution of counts issued by secondary pion (-) in the neutron monitor.



0

Figure 51 Distribution of counts issued by secondary photon in the neutron monitor.

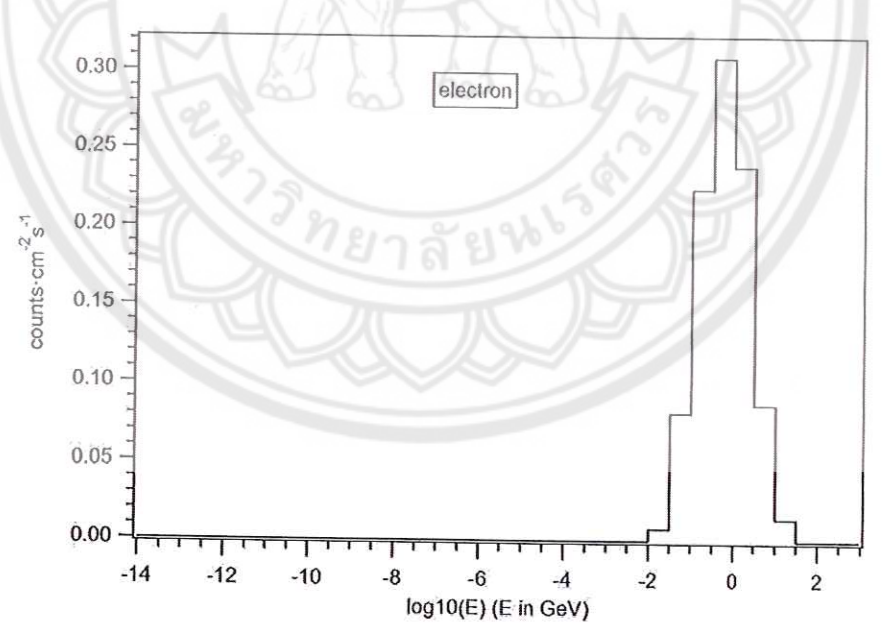


Figure 52 Distribution of counts issued by secondary electron in the neutron monitor.

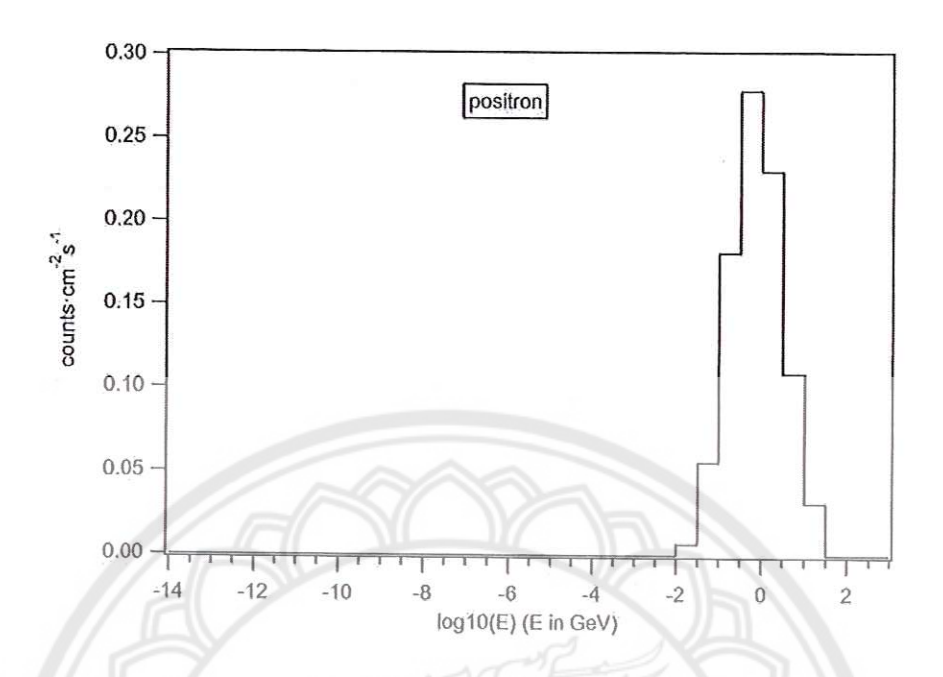


Figure 53 Distribution of counts issued by secondary positron in the neutron monitor.

The Figures 36-53 show the range of different energy for each particle with new weights, for which the count rate were detected by the calibration neutron monitor and the neutron monitor of the PSNM station. We found the patterns of flux distributions to be similar. Especially, the neutron distribution of both monitors have the neutron energy range from roughly 10 MeV to 10 GeV, with the main peak at 100 MeV. This simulation results show that the low-energy neutron (< 100 keV) are not enough to generate counts inside the monitor. Furthermore, we calculated the percentage of the secondary particles inside the neutron monitor and calibration monitor as shown in Table 10.

Table 10 Percentages of secondary particles in the neutron monitor and the calibration monitor.

Type of particles	Neutron monitor (%)	Calibration monitor (%)	
Neutron	$64.7163 \pm 0.0007$	$67.086 \pm 0.009$	
Proton	$24.168 \pm 0.002$	$20.35 \pm 0.03$	
Negative muon (μ <sup>-</sup> )	$3.787 \pm 0.004$	$3.16 \pm 0.06$	
Positive muon ( μ <sup>+</sup> )	$1.00 \pm 0.01$	$1.4 \pm 0.1$	
Negative pion (π <sup>-</sup> )	$0.98 \pm 0.01$	$0.5 \pm 0.1$	
Positive pion ( $\pi^+$ )	$0.92 \pm 0.01$	$0.5 \pm 0.1$	
Photon	$3.189 \pm 0.005$	$5.17 \pm 0.06$	
Electron	$0.64 \pm 0.01$	$0.9 \pm 0.1$	
Positron	$0.60 \pm 0.01$	$0.9 \pm 0.1$	

The majority of counts produced by neutrons were about 64.72% and 67.09% in the neutron monitor and the calibration monitor, respectively. The neutron count rate from the calibration monitor was more than the neutron count rates of the neutron monitor about 4% because <sup>3</sup>He gas in a proportional counter of the calibrator had a high cross section of gas which corresponded to high efficiency for neutron count rate more than BF<sub>3</sub>.

The generated protons in the neutron monitor and the calibration monitor were 24.17 and 20.4 respectively. The percentage of particles left will be counted when they have high enough energy for generating counts.

## Count rate as a function of height of calibration monitor and water below it

We simulated the calibration monitor with the secondary cosmic rays for all directions and all energies with the weight beam. It was designed similarly to the PSNM station's calibration. We studied the effect of the environmental reflection of particles into the calibration monitor by setting calibration monitor above the pool with two heights from the surface at 70 and 140 cm. We filled water in the pool to various heights of 0, 10, 20, 25, 30, 40, 50, 60 and 65 cm. The initial input values of this simulation were 400 runs of 10 million particles, and the initial size of area 380 cm × 440 cm which was 165 cm above the calibrator. The results of this simulation are summarized in Table 11 and Table 12, which consist of counts per cycle of neutron monitor (18NM64) and calibration monitor (CALMON) including the ratio of CAL/NM at calibrator heights of 70 cm and 140 cm from pool. The result of counts/cycle of neutron monitor with new weight beam was  $5.92 \times 10^3$  counts. The average of counts/cycle of the calibrator (at 70 cm) was approximately  $3.02 \times 10^{1}$ counts and the calibrator (at 140 cm) was 2.97 × 101 counts. The average ratios of CAL/NM were 0.00510(4) and 0.00501(4) for calibrator heights 70 cm and 140 cm respectively. These simulation results are shown in Table 11 and 12.

Table 11 Ratio of the count rate of the calibration monitor/neutron monitor at 70 cm calibrator height from pool.

Height of water	Counts/cycle		The ratio of	
(cm)	18NM64	CALMON	CAL/NM	
0	5918.894	30.338	0.00513(3)	
10	5918. 894	30.268	0.00511(4)	
20	5918. 894	29.817	0.00504(3)	
25	5918. 894	29.969	0.00506(3)	
30	5918. 894	30.064	0.00508(3)	
40	5918. 894	30.381	0.00513(4)	
50	5918. 894	30.135	0.00509(3)	
60	5918. 894	30.230	0.00511(4)	
65	5918. 894	30.382	0.00513(3)	

3.

Table 12 Ratio of the count rate of the calibration monitor/neutron monitor at calibrator height of 140 cm from pool.

Height of water	Counts/cycle		The ratio of
(cm)	18NM64	CALMON	CAL/NM
0	5918. 894	29.990	0.00507(4)
10	5918. 894	29.388	0.00497(3)
20	5918. 894	29.656	0.00501(4)
25	5918. 894	29.348	0.00496(3)
30	5918. 894	29.617	0.00500(3)
40	5918. 894	30.207	0.00510(4)
50	5918. 894	29.691	0.00502(4)
60	5918. 894	29.609	0.00500(3)
65	5918. 894	29.485	0.00498(3)

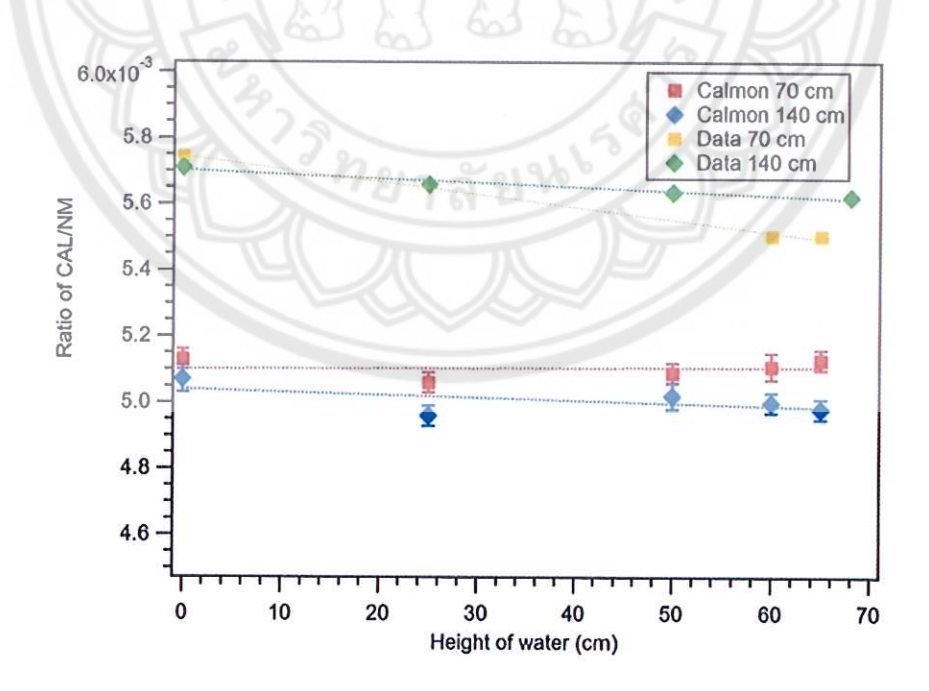
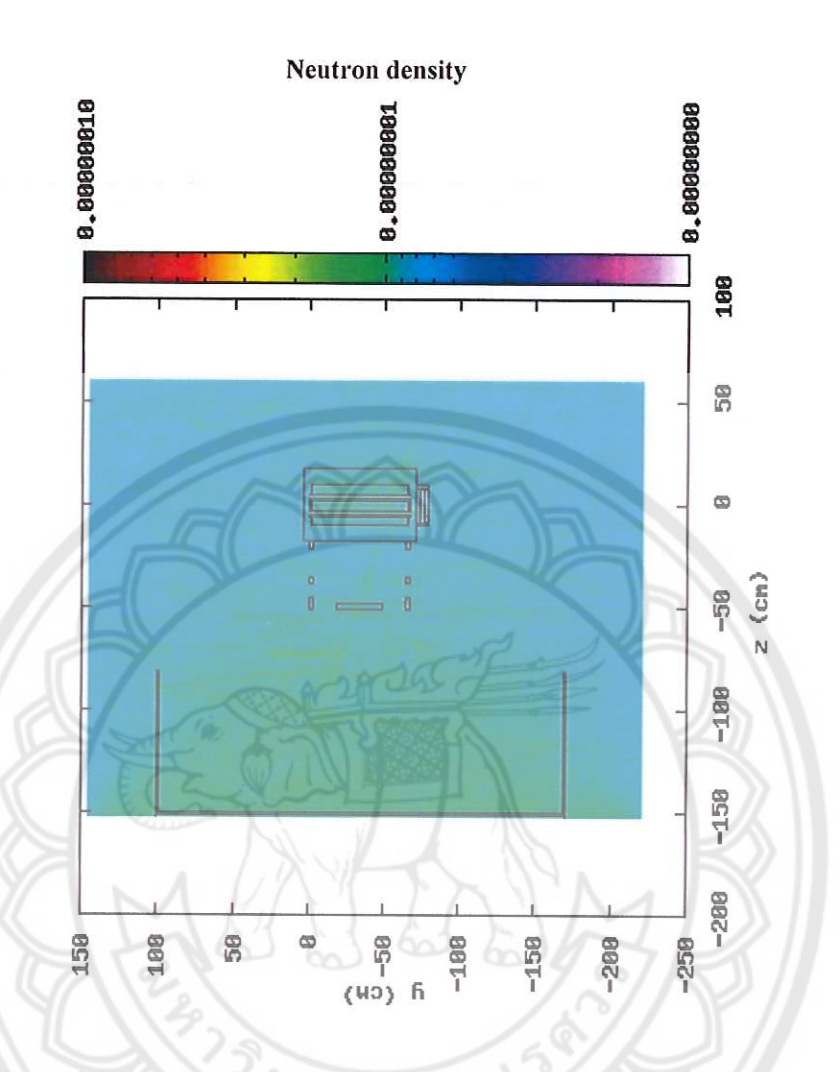


Figure 54 Comparison of the count rate ratio between simulations and experiments at the PSNM station for the calibrator and neutron monitor.

Figure 54 shows the comparison of count rates from simulations and experiments at the PSNM station at the heights of the calibrator at 140 cm and 70 cm. From the graph of the calibration monitor at 140 cm (blue line), we found its trend line of count rate, decrease 9 × 10<sup>-7</sup>/cm which this count rate decreases 1.78% of 65 cm, which corresponds to the experimental data (green line) with 1.58% decreasing. The percentage difference of CALMON vs experimental data at 140 cm is about 12%, because of the difference of the environment outside the calibration monitor. Therefore, count rate from the experiment is more than simulation. The CALMON simulation result at height 70 cm (red line) shows the count rate change for the various water heights are constant, while the result at height 140 cm shows a slight decrease of the count rate therefore the water height affects the neutron absorption as shown in Figure 55 and 56.



7

Figure 55 Neutron density plot on yz plane in the pool area for the calibrator at height of 140 cm without water.

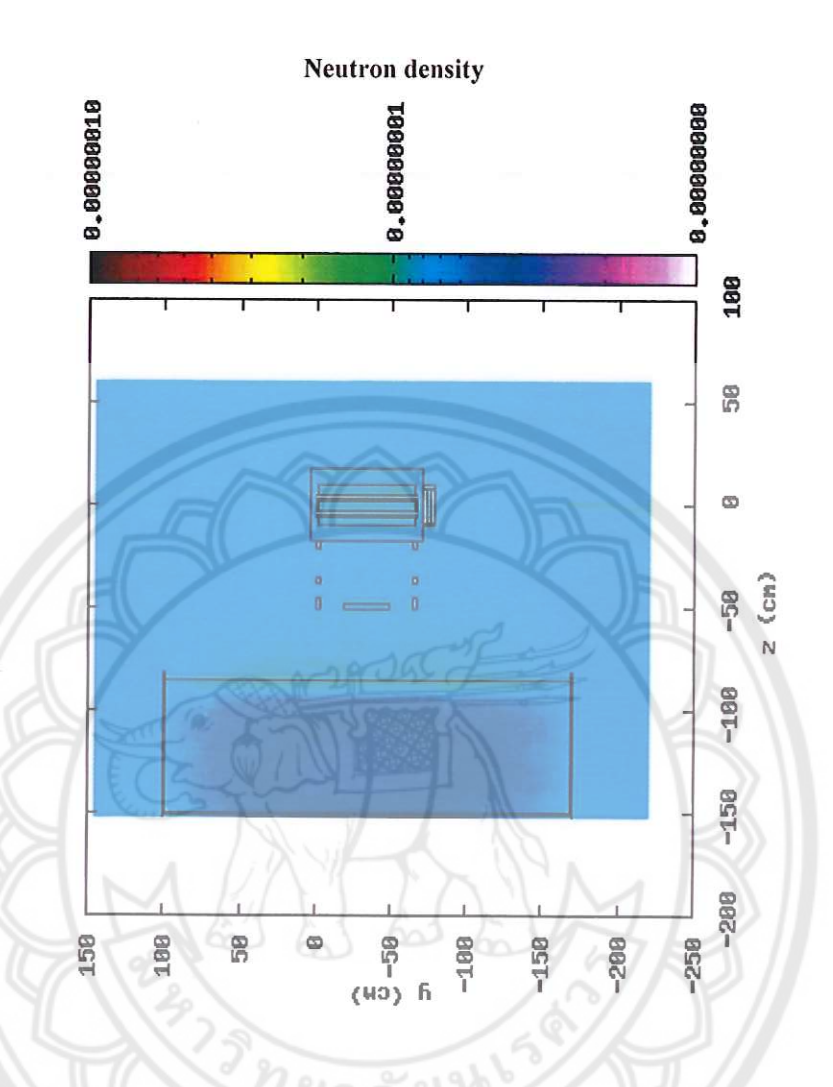


Figure 56 Neutron density plot on yz plane in the pool area for the calibrator at height of 140 cm above pool with water level at 65 cm.

Figure 55 and 56 show the neutron density in the empty pool and with water level at 65 cm by setting the height of calibrator at 140 cm. From the simulation result of the pool without water, the number of cloud neutrons splashed around the CALMON due to the effect of neutron scattering from the surface to the calibrator. We tried to decrease the cloud neutrons around the monitor by filling water to 65 cm level as shown in Figure 56. This is due to the fact that some of cloud neutrons are absorbed by the water. The detected count rates are the actual cosmic ray count rate.

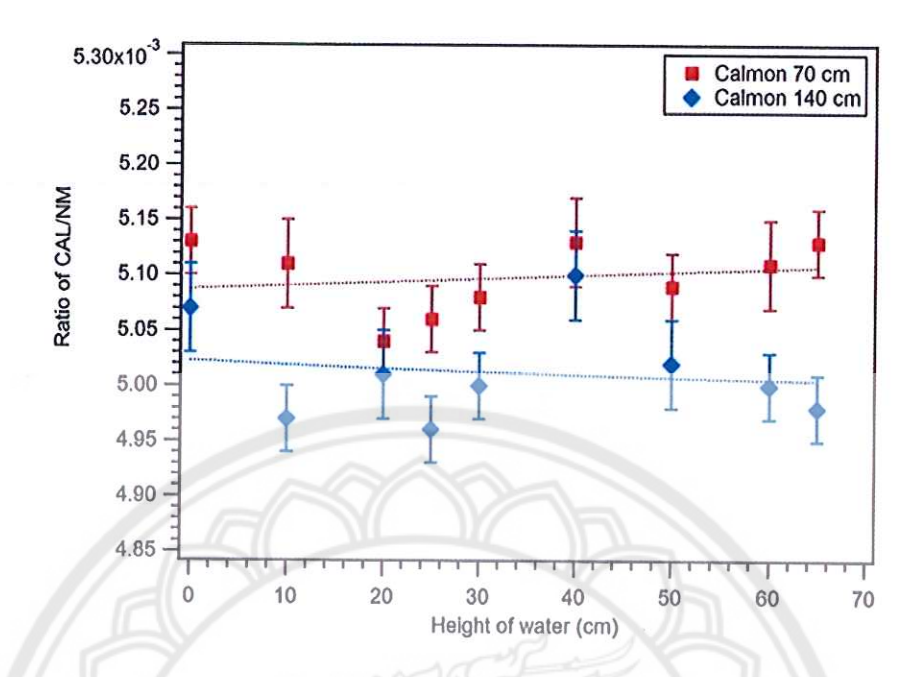


Figure 57 Count rate ratio as a function of height of calibration monitor for the calibrator and neutron monitor.

Figure 57 displays the count rates of the calibrator and neutron monitor as a function of height of calibration monitor with various water heights. We found count rates from the CALMON at height of 70 cm are more than those at 140 cm for every water height. We calculated the different percentage of the pool without water for both monitors to be approximately 1.18%. There are some neutrons that reflected into the lower height calibrator with greater solid angle of deflection.

## Count rates inside and outside the PSNM station

3

1)

In this section, we created the model of the CALMON, which was set up inside and outside of the PSNM station for comparing the count rates ratio of calibrator/18NM64. This simulated model inside station, there were 18 detectors in the neutron monitor, 3 bare counters and calibration neutron monitor which were set on concrete floor and all of them surrounded by concrete wall and roof. The positions of three monitors are shown in chapter 3.

In this FLUKA simulation, we used the input values of simulations at 330 runs (inside station) and 400 runs (outside station), 10 million particles with new weight beam. The starting beam area was  $1500 \times 1700$  cm<sup>2</sup>, and beam position at 600 cm from the ground. For the outside station simulation, we set the starting beam area at  $380 \times 440$  cm<sup>2</sup>, and beam position at 165 cm above the calibration monitor (540 cm from the ground). The inside and outside count rates from our simulation are shown in Tables 13-14.

Table 13 Ratio of the count rate inside vs outside the PSNM station.

Counts/cy		le	Ratio inside		Ratio outside
18NM64	CALMON	3Bare	3Bare/NM	CAL/NM	CAL/NM
5,919	31.56	119.11	0.0201(1)	0.0053(1)	0.00513(3)

Table 14 The ratio of the experimental count rate vs simulation count rate inside and outside station.

Inside station  Ratio of calibrator/neutron monitor		Outside station	
		Ratio of calibrator/neutron monitor	
experiment	simulation	experiment	simulation
0.005722(3)	0.0053(1)	0.005546(2)	0.00513(3)

From the simulation results for inside station, the counts/cycle of all three monitors were about  $5.92 \times 10^3$ ,  $3.16 \times 10^1$  and  $1.19 \times 10^2$  counts for neutron monitor, calibrator and bare counter, respectively. We got the count rate ratio of CAL/NM 0.0053(1) and the ratio of 3Bare/NM as 0.0201(1). Because the three monitors had different initial condition such as the filled gas ( $^{10}BF_3$  and  $^{3}He$ ), pressure, and operating voltage in the proportional counters (see Chapter 2), so the interactions between these particles and gas will affect the different count rate.

The count rate ratio comparison from our simulation in Table 13 showed that the difference in count rate ratio of inside and outside of CAL/NM is 0.00017(10). The ratio inside is about 3% more than outside. This is due to the effect of particle reflection from environment such as concrete walls, neutron monitor, concrete ground and door.

Tables 14 show the count rate ratio from the measurement and the simulation inside and outside the PSNM station. The difference in count rate ratio is only 0.0004 or  $\approx$  7%. We found that the difference between the ratio of CAL/NM inside and outside for the experiment to be (0.000176(4)), which is close to the simulation result of (0.00017(10)). Therefore, this simulation is in good agreement with the experiment.